WILEY-VCH

DOI: 10.1002/ ((please add manuscript number))
Article type: Full Paper

Compact 3D Copper with Uniform Porous Structure Derived by Electrochemical dealloying as Dendrite-free Lithium Metal Anode Current Collector

Heng Zhao, Danni Lei, Yan-Bing He*, Yifei Yuan, Qinbai Yun, Bin Ni, Wei Lv, Baohua Li, Quan-Hong Yang, Feiyu Kang and Jun Lu*

H. Zhao, Dr. D. N. Lei, B. Ni, Prof. W. Lv, Prof. B. H. Li, Prof. F. Y. Kang and Prof. Y. -B. He
Engineering Laboratory for the Next Generation Power and Energy Storage Batteries Graduate School at Shenzhen, Tsinghua University, Shenzhen, 518055, P. R. China.
E-mail: he.yanbing@sz.tsinghua.edu.cn
Q. B. Yun,
School of Materials Science and Engineering, Nanyang Technological University, Singapore, 639798, Singapore.
Prof. Q. -H. Yang
School of Chemical Engineering and Technology, Tianjin University, Tianjin, 300072, P. R. China.
H. Zhao, Dr. D. N. Lei, B. Ni and Prof. F. Y. Kang
Laboratory of Advanced Materials, School of Materials Science and Engineering, Tsinghua University, Beijing, 100084, P. R. China.
Dr. Y. Yuan; Prof. J. Lu
Chemical Sciences and Engineering Division, Argonne National Laboratory, Lemont, IL 60439, USA; E-mail: junlu@anl.gov

Keywords: electrochemical etching, 3D porous copper, Cu-Zn alloy, compact structure, Li metal batteries

Li metal anode of Li metal batteries is facing huge challenges such as uncontrolled Li dendrite growth and large volume change during Li plating/stripping, resulting in severe capacity decay and high safety hazards of batteries. 3D porous copper (Cu) current collector as host for Li deposition can effectively settle these problems. However, constructing uniform and compact 3D porous Cu structure is still an

enormous challenge. Herein, an electrochemical etching method for Cu-Zn alloy tape is reported to precisely engrave a 3D Cu with uniform, smooth and compact porous network. The continuous and compact 3D porous framework endows its excellent mechanical property and high electrical conductivity. The uniform and smooth pore with large internal surface area ensures well dispersed current density for homogeneous Li metal deposition and accommodation. A smooth and stable solid electrolyte interphase is formed and meanwhile the Li dendrites and dead Li are effectively suppressed. The Li metal anode conceived 3D Cu current collector can stably cycle for 400 h under a Li plating/stripping capacity of 1 mAh cm^{-2} and a current density of 1 mA cm^{-2}. The Li@3D Cu||$LiFePO_4$ full cells present excellent cycling and rate performances. The electrochemical dealloying is a robust method to construct 3D Cu current collector for dendrite-free Li metal anode.

1. Introduction

High energy density and long cycle life Li-ion batteries (LIBs) have promoted the wide applications and developments of mobile phones, laptops, renewable energy sources, electric vehicles, etc.[1-3] At present, the energy density of commercial LIBs, which use the graphite (372 mAh g^{-1}) as anode material, cannot meet the demands of electric vehicles.[4-9] Therefore, Li-sulfur batteries, Li-air batteries and lithium metal (Li-M) batteries with extremely high energy densities would play important roles in next-generation batteries.[10-20] As a component of these batteries, Li metal anode is considered as “Holy Grail” because of its high capacity (3800 mAh g^{-1}), low voltage

(-3.04 V vs standard hydrogen electrode) and small density (0.53 g cm^{-3}) as key factors to achieve high energy density of batteries.[21-23] However, several disadvantages, such as Li dendrite growth,[24] dead Li formation,[25] low Coulombic efficiency (CE),[26] high reactivity and uncontrolled volume expansion,[27] limit the application of Li metal anode, especially the dendrite growth and volume expansion during Li plating/stripping process.

Great efforts have been made to suppress the Li dendrite growth and volume expansion.[28-29] Constructing a stable solid electrolyte interface (SEI) layer on Li anode is an effective way to suppress the Li dendrite growth and reduce the side reactions between the electrolyte and Li metal anode.[30] Electrolyte additives can also reinforce surface stability of the Li metal anode, including $LiPF_6$,[31] fluoroethylene carbonate (FEC),[32] vinylene carbonate (VC),[33] inert cation (Cs^+, Rb^+),[34] phosphorous pentasulfide[35] and even trace amount of water.[36] In addition, using solid electrolytes is an effective way to tackle the challenges of the Li metal anode.[37-38]

Although the protective coating layers, electrolyte additives and various electrolytes can stabilize the Li metal anode and suppress the Li dendrite growth to some extent, they cannot prevent the expansion/shrink of the Li metal anode during charge/discharge process, which is another major obstacle to practical application of Li metal anode. Therefore, researchers developed many stable hosts to accommodate the Li deposition and minimize the volume change of Li metal anode, including layered reduced graphene oxide,[39] 3D current collector,[26] 3D carbon nanotube

sponge,[40-41] 3D nickel foam,[42] etc. Copper (Cu) is the most commonly used current collector in the LIBs industry, and several work reported the usage of porous Cu current collectors to accommodate Li deposition and suppress the dendrite growth, such as nanoporous free-standing Cu nanowire network,[43] 3D Cu mesh,[44] 3D porous Cu foil,[26] etc. These obtained 3D structures can efficiently prevent the dendrite growth and Li expansion. However, the large-scaled and precisely-controlled production of these 3D structures is still challenging. In addition, some 3D Cu current collectors are too thick to be applied in the battery industry because it will greatly lower the energy and volume density of batteries. In our previous work, a Cu current collector with 3D porous structure was produced by a simple chemical dealloying process of Cu-Zn alloy for Li metal anodes.[45] The voids in the 3D current collector can effectively accommodate Li deposition and suppress the Li dendrite growth. Unfortunately, it is difficult to precisely regulate the pore structure of the 3D Cu current collector to achieve uniform porous structure during the chemical dealloying process, and meanwhile the 3D Cu presents poor mechanical strength and low electrical conductivity due to the relatively loose structure. The electrochemical etching of a more active component from a homogeneous alloy has become a significant method for tuning the structure and morphology of high surface area porous materials.[46-47] This method is a green and controllable method which can precisely engrave uniform and smooth porous structure.

In this work, we report a compact 3D Cu current collector with uniform and smooth porous structure derived from a novel electrochemical etching method of a Cu-Zn alloy

tape by linear sweep voltammetry (LSV) (**Figure 1**a). The 3D Cu consists of abundant and uniform pores as well as a compact 3D Cu framework, which endows 3D porous Cu highly enhanced mechanical property. This novel 3D Cu architecture offers several unique advantages as current collector of Li metal anode (Figure 1b). Firstly, the pores with uniform and proper size cooperated with the smooth pore surface contribute to the formation of a high-quality SEI layer on the top and inside pores of the 3D Cu, thus the side reactions between Li anode and electrolyte can be effectively reduced. Secondly, the uniform pores enable the small and well-distributed current density inside 3D Cu, resulting in low polarization and uniform Li plating/striping inside pores to effectively suppress the Li dendrites and accommodate the Li deposition. Thirdly, the good mechanical strength brings up the high structural stability of the Li@3D Cu (the 3D Cu current collectors deposited with Li) composite electrode during long cycling. The assembled Li||Li@3D Cu (Li was used as anode and Li@3D Cu as cathode) cells with such unique 3D Cu current collector present considerably stable cycling performance. Especially, no short circuits of Li||Li@3D Cu cells occur even after cycling for 400 h under a high Li plating/stripping capacity of 1 mAh cm^{-2} and current density of 1 mA cm^{-2}. Moreover, the Li@3D Cu||$LiFePO_4$ (the 3D Cu current collectors deposited with Li were used as anode and $LiFePO_4$ as cathode) full cells present excellent cycling and rate performances. On the contrary, uncontrolled dendrites are formed on the 2D Cu current collector, together with constantly produced dead Li and unstable SEI layer, resulting in low CE, poor life span and large volume expansion of Li@2D Cu anode. This work can promote the mass production of 3D Cu current collector with uniform

structure, which would boost the application of Li metal anode for the next-generation batteries.

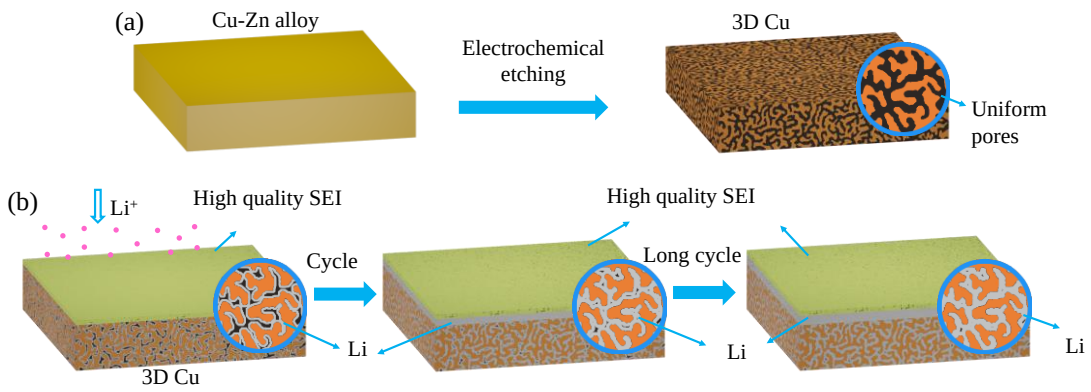

Figure 1. (a) Schematic of electrochemical etching of Cu-Zn alloy tape to prepare the 3D Cu current collector; (b) Li deposition on the 3D Cu current collector during cycling.

2. Results and Discussion

The 3D porous Cu collector was fabricated by electrochemical etching of brass tape ($Cu_{0.64}Zn_{0.36}$) using linear sweep voltammetry (LSV) between -1 and 0.2 V. The sample (**Figure 2**a and b) after electrochemical etching shows the color of Cu. The X-ray diffraction (XRD) analysis in Figure 2c shows that, with the increase of LSV cycles, the peak intensity of $Cu_{0.64}Zn_{0.36}$ phase decreases and the characteristic peaks of the Cu phase become stronger, suggesting that the Zn element is removed gradually from the pristine Cu-Zn alloy and pure porous Cu tape can be obtained after 50 LSV cycles (Figure S1). The stress-strain curves in Figure 2d show that the electrochemical etched 3D Cu current collector presents good mechanical property, whose tensile strength is 13.5 MPa, which is three times larger than that of 3D Cu current collector obtained by chemical dealloying process. This enhanced mechanical strength can

improve the structural stability of the Li anode during cycling, and is beneficial for mass production for practical application. In additon, the electrical conductivity of Cu-Zn alloy is 1.39×10^{5} S cm^{-1} and that of electrochemical etched 3D Cu is 1.12×10^{5} S cm^{-1}, which is much higher than that of chemical dealloyed 3D Cu (1.31×10^{4} S cm^{-1}). Thus, the electrochemical dealloying for Cu-Zn alloy almost does not damage its electronic conductive network.

The SEM image in Figure 2e shows that Cu-Zn alloy before electrochemical etching presents a compact and solid structure. The $Cu_{0.64}Zn_{0.36}$ alloy has a quite homogeneous Cu and Zn distribution as shown in Figure 2e-g, which is very important for fabricating the compact 3D Cu with uniform porous structure. After electrochemical etching with 50 LSV cycles, a uniform porous structure was formed throughout the whole sample (Figure 2h). The element mapping results present that Cu is still uniformly dispersed as that in pristine Cu-Zn alloy tape but Zn almost disappears (Figure 2f, g, i, j and Figure S2). These results suggest that a uniform porous 3D Cu skeleton structure can be fabricated using the controllable electrochemical etching method. The high-resolution SEM images of the Cu-Zn tape after electrochemical etching clearly show that a 3D interlinked and smooth porous network with uniform pore size around 1 μm was formed (**Figure 3**a and b). This homogeneous and compact 3D porous structure is expected to provide low and well-distributed current density for uniform Li deposition, thus suppressing the formation of Li dendrites. The calculated porosity of the prepared 3D Cu is 44.3 % according to Formula 1 in Experimental section. The abundant pores and voids in this

3D Cu current collector can well accommodate Li deposition, thus buffering the severe volume change of Li anode during Li plating/stripping and ensuring a stable electrode/electrolyte interface. Moreover, such a highly porous structure has much smoother and more continuous pores compared to that of the 3D Cu current collector produced by chemical dealloying method,[45] which may result in more even current distribution and more uniform Li deposition. The lower resistance of fresh electrochemical etched 3D Cu based-coin cell may be attributed to the higher electron conductivity of electrochemical etched 3D Cu current collector (Figure S3a).

From the morphology of samples treated with different LSV cycles, it is observed that the etching process starts from the surface to the interior of Cu-Zn alloy tape (Figure S4) and the pore structure can be controlled by adjusting the electrochemical etching time. It should be noted that the etching reaction would begin at the sites contacting electrolyte during LSV. At initial etching, the electrolyte contacted the surface of both sides of Cu-Zn alloy tape, suggesting that the etching reaction occured from the surface of both sides of Cu-Zn alloy tape and then gradually to the interior of Cu-Zn alloy tape. In addition, the two nickel foam counter electrodes were faced on both sides of Cu-Zn alloy tape working electrode, which promoted the uniform etching from both surface of Cu-Zn alloy tape.

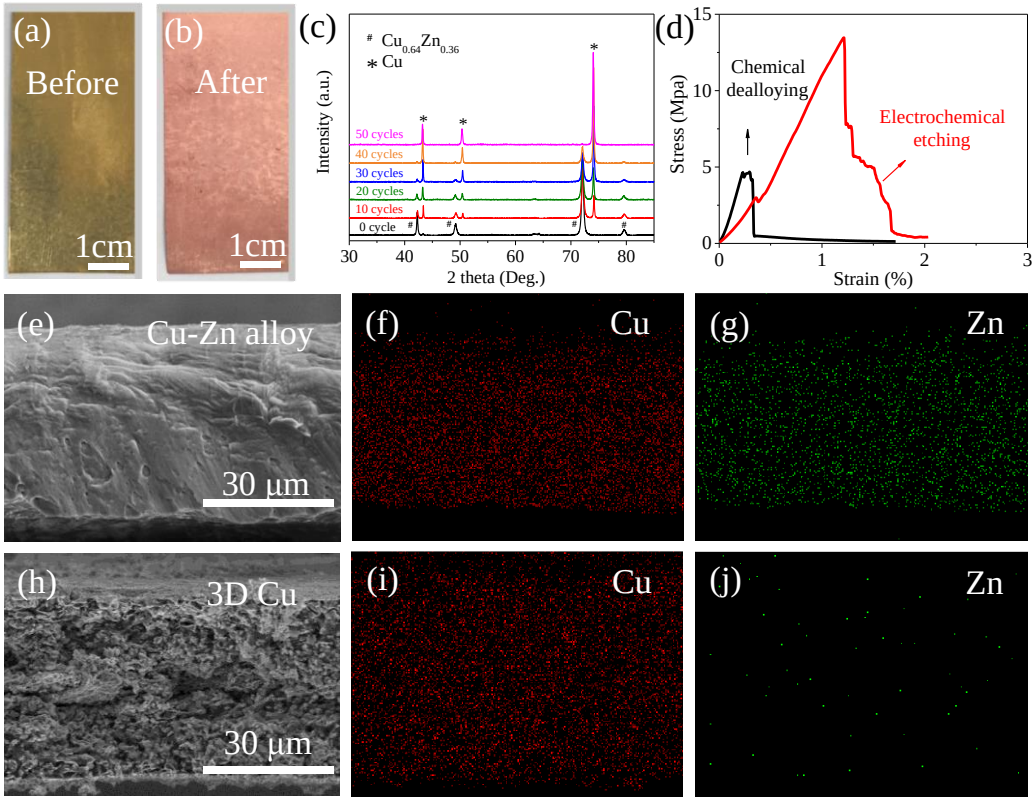

Figure 2. Photo images of (a) Cu-Zn alloy tape and (b) as-prepared 3D Cu current collector; (c) XRD patterns of Cu-Zn alloy and 3D Cu current collector with different LSV cycles; (d) Stress-strain curves of 3D Cu current collectors prepared by chemical dealloying method and electrochemical etching method; Cross-view SEM image of (e) Cu-Zn alloy and (h) 3D Cu current collector; Element mapping picture of Cu and Zn in (f, g) Cu-Zn alloy tape and (i, j) as-prepared 3D Cu current collector.

In order to investigate the Li deposition behavior in electrochemical etched 3D Cu, the morphology of the 3D porous and 2D plate Cu before and after different Li plating/stripping cycles was examined by SEM (Figure 3). The 3D porous Cu and 2D Cu current collectors were cycled for different times with Li plating/stripping of 2 mAh cm^{-2} at a current density of 1 mA cm^{-2}. It is seen from Figure 3c and g that the thickness of Li deposition and SEI layer on the top of 2D Cu current collector is 16.3 μm after 10 cycles, which is much larger than that of 3D porous Cu current collector with thickness of 8.1 μm (Figure 3a and e). This Li deposition behavior indicates that

a large amount of Li was deposited inside of 3D porous Cu, which can be further proved by the morphology changes of the pore structure of 3D Cu current collector after Li deposition. Comparing the inset SEM images of Figure 3a and e, it can be observed that the void space in 3D porous Cu becomes much smaller and smooth as well as uniform Li is deposited on the Cu framework. These results suggest that the interlinked porous structure ensures a high electrical conductivity of the current collector and enables the electrolyte to wetting inner surface of 3D porous Cu, resulting in homogeneous Li deposition. Considering the porosity of the as-prepared 3D current collector, Li would fill 60 % of the voids in 3D Cu current collector when 2 mAh cm^{-2} of Li is deposited inside 3D porous Cu. Nitrogen adsorption/desorption measurements of 3D porous Cu before and after Li deposition present a decrease in both Brunauer-Emmett-Teller (BET) specific surface area (from ~1.430 m^2 g^{-1} to ~0.277 m^2 g^{-1}) and pore volume (from ~0.0056 cm^3 g^{-1} to ~0.0027 cm^3 g^{-1}) (Figure S5a-b). The Li filling ratio of pores reaches ~50 % according to the decrease of pore volume, which is very close to the theoretical value, indicating that Li was confined into the pores of 3D Cu successfully. It is also worth to note that the specific surface area of 3D Cu is 110 times higher than that of 2D Cu (0.013 m^2 g^{-1}, calculated according to the Formula 2) resulting in the low and uniform current dispersion thus no dendrite formation.

From the SEM images of top view of 3D Cu before and after cycling (Figure 3b and f), it can be observed that a smooth and dense deposition layer was formed on the top surface of 3D Cu. In contrast, the deposition layer on the top of 2D Cu cracked

and a large amount of Li dendrites were formed (Figure 3h). When the cycle number increased to 100 cycles, the very smooth, uniform and dense Li and SEI layer can maintain on the top of 3D porous Cu and no Li dendrites were formed (Figure 3j). The thickness of Li and SEI layer only increased slightly to around 12.6 μm (Figure 3i). However, a more porous, cracked and thicker Li and SEI hybrid layer with thickness as large as 32.1 μm was formed on the top of 2D Cu (Figure 3k and l), which can be ascribed to the formation of a large amount of dead Li and SEI layer.[44, 48-49] Such observation indicates that the lower and well-distributed current density in 3D porous Cu current collector leads to the uniform Li disposition inside the continuous and smooth 3D Cu porous network. The abundant and uniform pores and voids in this 3D Cu current collector can well accommodate Li deposition and alleviate the severe volume change of Li anode during Li plating/stripping. Thus, a stable electrode/electrolyte interface is formed and Li dendrite growth is effectively suppressed. At the same time, from the comparison of the channel morphology of porous 3D Cu after 10 and 100 cycles (inset of SEM images in Figure 3e and i), it can be seen that the deposited Li layers have similar, smooth and very stable structures after cycling, indicating high reversibility of Li plating/striping process in prepared 3D Cu current collector with uniform porous network. The much smaller resistances of cycled porous Li||Li@3D Cu cell than that of Li||Li@2D Cu cell as shown in Figure S3b further confirm the high cycling reversibility of 3D Cu with uniform porous network, in which a stable electrode structure and SEI layer can be achieved.

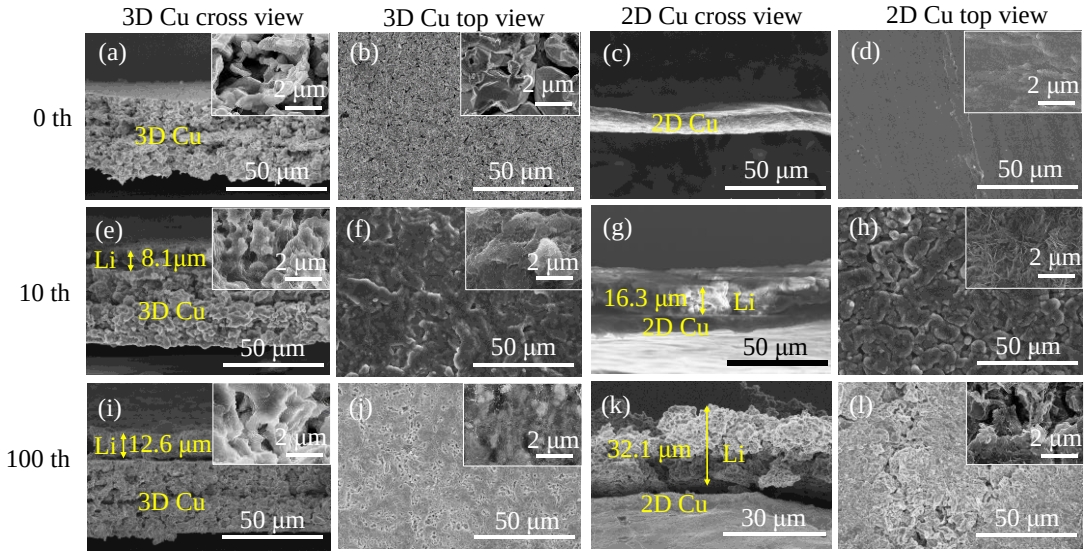

Figure 3. SEM images of 3D and 2D Cu current collectors before and after Li deposition of a total capacity of 2 mAh cm^{-2} with a current density of 1 mA cm^{-2}: (a, b) fresh 3D Cu, (c, d) fresh 2D Cu, (e, f) 3D Cu after 10 cycles, (g, h) 2D Cu after 10 cycles, (i, j) 3D Cu after 100 cycles, (k, l) 2D Cu after 100 cycles. The insets are corresponding high-magnification SEM of each image.

The 3D Cu and 2D Cu current collectors were cycled at the current density of 1 mA cm^{-2} with plating/stripping capacity of 1 mAh cm^{-2} to investigate the reversibility of Li@Cu anodes. The voltage profiles of both 2D and 3D Cu based cells have similar shapes, while the 2D Cu shows larger polarization than 3D Cu. The voltage gap between charge and discharge plateaus of 2D Cu is ~0.21 V for 1st cycle, which is much larger than that of 3D Cu (~0.09 V) (**Figure 4**a,b). The stable voltage gap between charge and discharge plateaus of 2D Cu during the following cycles (~0.14 V) is also obviously larger than that of 3D Cu (0.09 V). Additionally, the voltage gap of as-prepared 3D Cu using electrochemical etching at current density of 1 mA cm^{-2} (0.09 V) is even smaller than that of chemical dealloyed 3D Cu current collector (0.1 V) at current density of 0.5 mA cm^{-2}.[45] What's more, the deposition of Li metal onto 3D Cu current collector has much smaller nucleation overpotential (-0.099 V) than 2D

Cu current collector (-0.214 V), which indicates that 3D Cu current collector greatly favors the Li deposition (Figure S6).[50-51] Such smaller polarization in electrochemical etching derived 3D Cu current collector can be attributed to following reasons. First, the porous 3D Cu has smaller Li deposition resistance resulted from its interlinked uniform pores with large surface area. Second, in the porous 3D Cu structure, numerous protuberant tips exist, which act as the charge centers and nucleation sites for lithium uniform deposition.[26] The lithium nucleation sites for porous 3D Cu are much more than that of the flat 2D Cu current collector. A homogeneous SEI layer is formed on both inner and outer surface of 3D Cu, which makes the Li ions uniformly and mildly pass through the SEI layer.

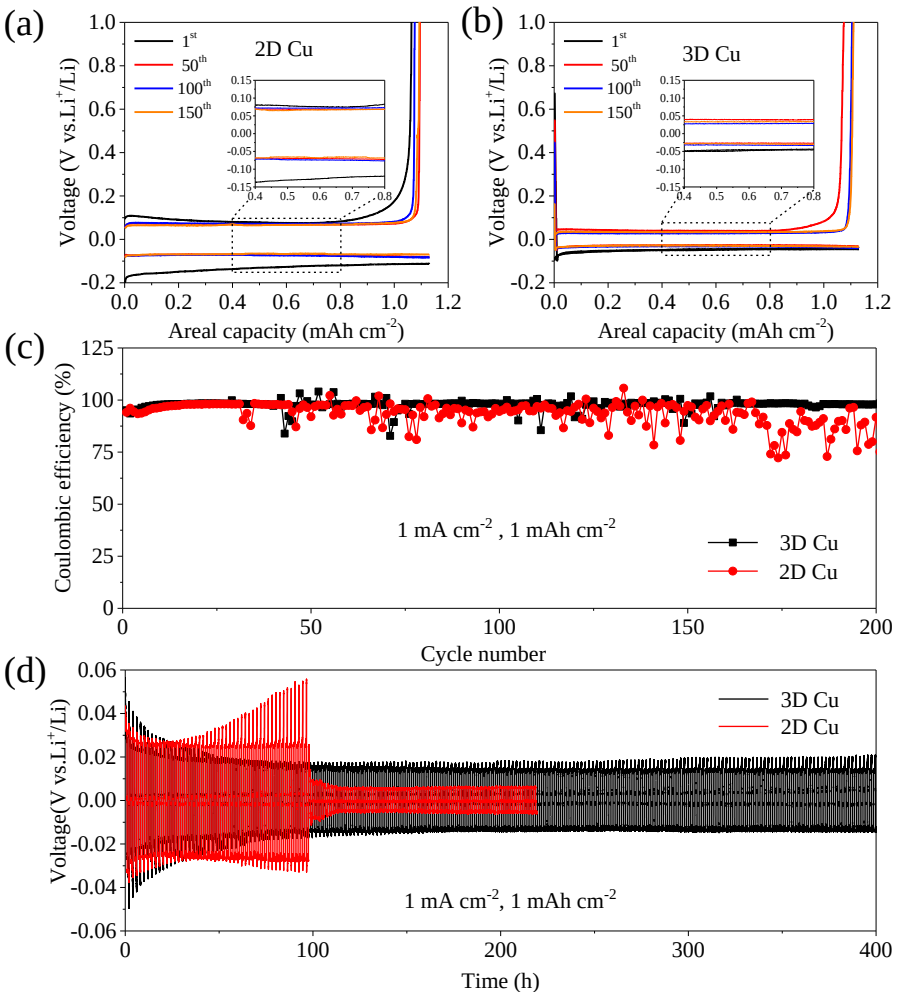

Figure 4. Electrochemical performance of 2D and 3D Cu current collectors: (a,b) Voltage profiles of Li plating/stripping on (a) 2D and (b) 3D Cu current collectors with a current density of 1 mA cm^{-2} for a total Li deposition of 1 mAh cm^{-2}; (c) Coulombic efficiencies of Li plating/stripping on 2D and 3D Cu current collectors with current density of 1 mA cm^{-2} for a total Li deposition of 1 mAh cm^{-2}; (d) Cycling performances of Li||Li@Cu cells using 2D and 3D Cu current collectors with a Li plating/stripping for 1 h at current density of 1 mA cm^{-2}.

From Figure 4c, it is demonstrated that the CE of produced 3D porous Cu current collector quickly increases to above 90 % in initial cycles and stably retains over 97.9 % after 200 cycles. In contrast, the CE of 2D Cu current collector shows severe fluctuation, which indicates that the SEI on the 2D Cu current collector is unstable and continuously formed during cycles due to the formation of Li dendrites and dead

Li (Figure 3k, l).[26, 52] Moreover, a higher CE was observed in the 3D Cu current collector using electrochemical etching than chemical dealloying method.[45] This can be ascribed to the unique porous structure of 3D Cu current collector by electrochemical etching, where less current density concentration is formed since its more uniform and interlinked pores are able to fast disperse electrons and achieve homogeneous Li deposition. These results are highly consistent with the observation in SEM studies (Figure 3e, f, i, j). In addition, compared with chemical dealloyed 3D Cu current collector, the better mechanical strength of electrochemical etched 3D Cu current collector could result in better structural stability of the whole electrode during long cycles (Figure 2b). Thus, the electrochemical etching method is more competitive in the future application.

The long cycling performance of Li||Li@Cu cells was checked to further evaluate the performance of the 2D and 3D Cu current collectors (Figure 4d). The 2D and 3D Cu current collectors were cycled under a current density of 1 mA cm^{-2} with a high Li plating/stripping capacity of 1 mAh cm^{-2}. Even after 400 h, the Li plating/stripping polarization of 3D Cu current collector was stabilized at ~20 mV and no short circuit was observed. This is one of the longest time under a high Li plating/stripping capacity of 1 mAh cm^{-2} and current density of 1 mA cm^{-2} compared to other current collectors as shown in Table S1. On the contrast, the polarization of 2D Cu current collector is not stable and much larger than that of 3D Cu current collector. These results indicate that the 3D Cu current collector presents exellent cycling reversibility of Li plating/stripping and the Li dendrite growth has been successfully suppressed,

which result in a stable SEI layer. Such excellent performance of 3D porous Cu current collector further proves that the proper pore size and uniform pore structure in 3D Cu is very singnicant and necessary for the uniform Li deposition and accommodation, which is able to alleviate the severe volume change of Li anode during cycling.[52]

Li@Cu||$LiFePO_4$ full cell test was adopted to evaluate the commercial application of 3D Cu current collector. From **Figure 5**a, it can be seen that the $LiFePO_4$ of 3D Cu current collector based full cell exhibits relatively higher capacity after 350 cycles at 1C than that of 2D Cu current collector based full cell (127.5 mAh g^{-1} vs. 119.9 mAh g^{-1}). The excellent cycling performance of Li@3D Cu||$LiFePO_4$ indicates that the Li@3D Cu possesses high structural stability for long cycling, which can be ascribed to the good mechanical strength of 3D Cu with continuous and compact inner wall of pores, as well as the suppressed Li dendrite growth due to the even Li deposition in the uniform pores of 3D Cu. Therefore, Li@3D Cu is an efficient and stable anode for full batteries. More importantly, the rate performance of 3D Cu current collector is much better than that of 2D Cu (Figure 5b). The specific capacities of Li@3D Cu||$LiFePO_4$ at 0.3 C and 4 C are 146.4 and 115 mAh g^{-1}, respectively, which are much larger than that of Li@2D Cu||$LiFePO_4$ cells (122.3 and 83.5 mAh g^{-1}). Even at a high rate of 20 C, the Li@3D Cu||$LiFePO_4$ cell delivers a capacity of 70 mAh g^{-1}, while the capacity of Li@2D Cu||$LiFePO_4$ is only 15 mAh g^{-1}. The improved rate performance of Li@3D Cu||$LiFePO_4$ can be ascribed to the fast electron and Li^+ transport in Li@3D Cu anode. Moreover, the voltage hysteresis of

Li@3D Cu||$LiFePO_4$ at various charge/discharge rates is obviously smaller than that of Li@2D Cu||$LiFePO_4$ as shown in Figure 5c and d. The much better rate performance and smaller voltage hysteresis indicate the obviously smaller polarization of Li@3D Cu than that of Li@2D Cu. After Li deposition into 3D Cu with uniform porous structure, the surface area of Li greatly increased, thus resulting in the reduction of the polarization of Li@3D Cu anode and the improvement of the kinetic properties. In addition, it is seen from Figure 5a and b that the Li@3D Cu||$LiFePO_4$ cells present very stable CE during cycling and rate tests. In all, the uniform porous 3D Cu current collector with high mechanical strength endowed the excellent cycling and rate performances of Li@3D Cu||$LiFePO_4$.

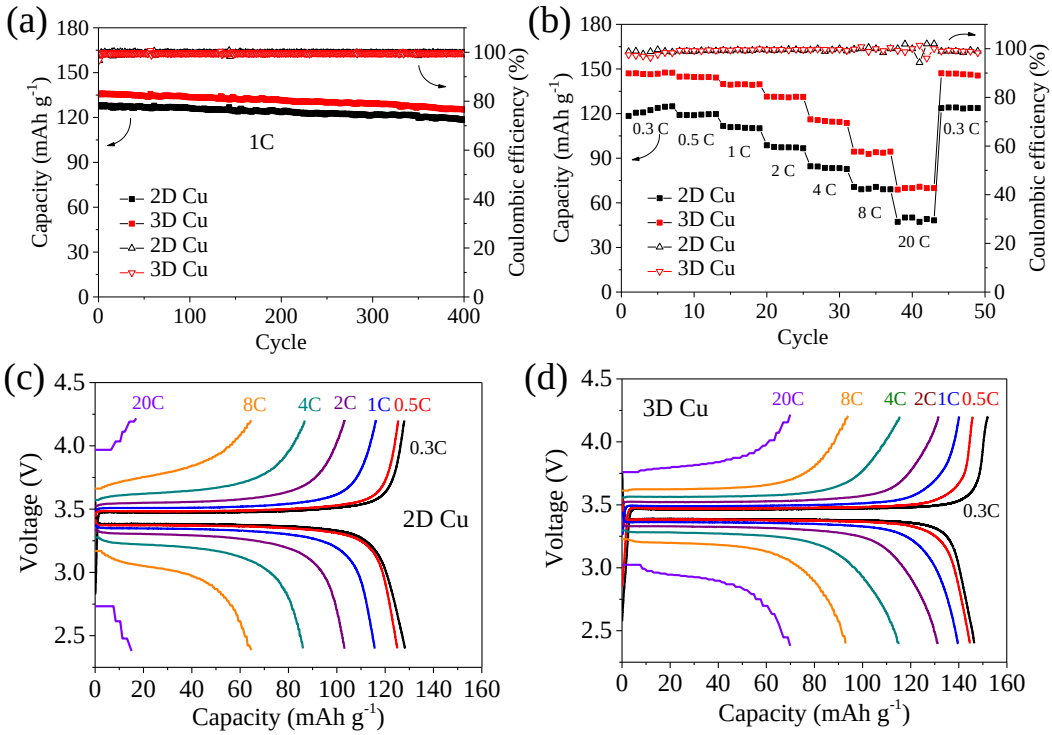

Figure 5. Cycling and rate performances of full cells using 2D(a) and 3D(b) Cu current collectors; Charge and discharge curves of full cells under different rates using 2D(c) and 3D (d) Cu current collectors.

3. Conclusion

In summary, a compact 3D Cu current collector with uniform and smooth porous structure was prepared for Li metal batteries by an easily manipulated, low-cost LSV electrochemical etching approach of the Cu-Zn tape. The uniform and smooth 3D Cu porous network provides well-distributed current density for homogeneous Li metal deposition and accommodation. A smooth and stable SEI film is formed on and inside the 3D Cu to effectively improve the CE of Li plating/stripping and suppress Li dendrite growth. The continuous and compact 3D porous framework endows much highly enhanced mechanical property to ensure a long cycling life at high current densities. The Li metal anode with such compact and uniform 3D porous current collector can stably cycle for as long as 400 h under a high Li plating/stripping of capacity of 1 mAh cm^{-2} and high current density of 1 mA cm^{-2}. Moreover, the Li@3D Cu||$LiFePO_4$ full cells also present excellent cycling and rate performances. This work provides a novel and controllable electrochemical etching approach to large-scaled production of 3D Cu current collector with well-knit and uniform porous structure, which would effectively boost the commercial application of Li metal batteries.

4. Experimental Section

Fabrication of 3D porous current collector: Linear sweep voltammetry (LSV) method was used to accurately remove Zn from the Cu-Zn alloy tape under the sweeping speed of 1 mV s^{-1} with the voltage window between -1 and 0.2 V in a three electrode system. A brass tape (40 μm in thickness) was firstly washed by alcohol to remove

pristine contaminations and then used as working electrode. Saturated calomel electrode was used as reference electrode and nickel foam was used as counter electrode. Two nickel foam counter electrodes were faced both sides of Cu-Zn Alloy working electrode. HCl solution of 0.125 mol L^{-1} was prepared as electrochemical etching electrolyte. By controlling the cycles of electrochemical etching process, 3D porous Cu current collector was fabricated. After that, the samples were rinsed with deionized water and dehydrated alcohol for 3 times. To prepare 3D current collectors for Li metal anode, the 3D porous Cu was dried in a vacuum chamber at 60 °C for 6 h and punched into circular disks with a diameter of 12 mm.

Structure characterization: X-ray diffraction patterns of Cu-Zn alloy before and after electrochemical dealloying were collected on a Rigaku D/MAX 2500/PC diffractometer using Cu Kα radiation. Scanning electron microscope (SEM) and energy dispersive spectroscopy (EDS) were recorded on a FE-SEM (HITACH S4800) at 15 kV. The nitrogen adsorption/desorption isotherms of 3D Cu before and after Li deposition (2 mAh cm^{-2}, 1 mA cm^{-2} for 3 cycles) were obtained at 77 K by using an automated adsorption apparatus (Micromeritics ASAP 2020) and the surface area was calculated based on the Brunauer-Emmett-Teller (BET) equation. Stress-strain tests for the chemical dealloyed and electrochemical etched 3D Cu current collectors were performed by using a CMT6104 tensile testing machine. The electrical conductivity of Cu-Zn alloy before and after chemical dealloying and electrochemical dealloying were measured using the four-point probe method (LORESTA GP, MCPT610).

The porosity of as-prepared 3D current collector was calculated according to the

below formula:

$$P = \left(\frac{V_1 - V_2}{V_1}\right) \times 100\ \% \quad (1)$$

V_1: volume of 3D porous Cu

V_2: volume of commercial 2D Cu

The specific surface area (SSA) of 2D Cu was calculated according to the below formula:

$$SSA = \frac{\pi r^2 + \pi * 2r * d}{m} \quad (2)$$

r: radius of 2D Cu electrode

d: thickness of 2D Cu electrode

m: weight of 2D Cu electrode

Electrochemical measurements: To test CE, electrochemical impedance spectrum(EIS) and other performance, CR2032 coin cells were assembled using Li metal foil as counter electrode, 2D or 3D Cu current collector as the working electrode, polypropylene film as the separator, 60 μL electrolyte of 1 M lithium bis(trifluoromethanesulonyl)imide (LiTFSI) in 1,2-dimethoxyethane (DME) and 1,3-dioxolane (DOL) was used for each cell. All the batteries were assembled in Ar-filled glove box and tested on a LAND-CT2001A cell test instrument at 25 °C. Before the formal testing, coin cells were cycled for 5 cycles from 0 to 1 V at 50 μA to stabilize the interface and remove surface contaminations.[53] The voltage profile of 3D Cu coin cells in this process can be seen in the Figure S7. To characterize the morphology of Li deposition, the coin cells were disassembled after 10 cycles and 100 cycles with Li plating/stripping of 2 mAh cm^{-2} at a current density of 1 mA cm^{-2}.To

test CE, a fixed amount of 1 mAh cm^{-2} of Li was deposited on the current collector and then cycled with current density of 1 mA cm^{-2}. EIS measurements were tested from 100 kHz to 10 mHz with the amplitude of 5 mV using a VMP3 multichannel electrochemical station (Bio Logic Science Instruments, France). During the polarization test, the Li||Li@Cu cells were charged/discharged at 1 mA cm^{-2} for 1 h in each cycle after 3 mAh cm^{-2} of Li was deposited on the current collector. Li@Cu||$LiFePO_4$ full cells were assembled using $LiFePO_4$ as cathode while Li@Cu (Li deposited on the Cu current collectors) used as anode. Li@Cu was prepared after 1 mAh cm^{-2} Li deposited on the 2D or 3D Cu current collectors, these half cells were then disassembled in the Ar-filled glove box and at the same time Li@Cu was reassembled in full cells as anode. $LiFePO_4$ electrode was provided by Shenzhen Dynanonic Co., Ltd. The electrolyte used in full cells is the same with that in half cells. All the full cells were cycled between 2.4 and 4.2 V during the cycling and rate tests.

Supporting Information

Supporting Information is available from the Wiley Online Library or from the author.

Author contribution:

H. Zhao and D. Lei contributed equally to this work.

Acknowledgements

This work was supported by the National Key Basic Research Program of China (2014CB932400), the National Natural Science Foundation of China (51672156 and 51232005), Guangdong special support program (2015TQ01N401), Guangdong Province Technical Plan Project (2017B010119001 and 2017B090907005), Dongguan City (2015509119213), Shenzhen Technical Plan Project (KQJSCX20160226191136, JCYJ20170412170706047，JCYJ20170307153806471 GJHS20170314165324888). J. Lu gratefully acknowledges support from the U. S. Department of Energy (DOE), Vehicle Technologies Office. Argonne National Laboratory is operated for DOE Office of Science by UChicago Argonne, LLC, under contract number DE-AC02-06CH11357.

Received: ((will be filled in by the editorial staff))
Revised: ((will be filled in by the editorial staff))
Published online: ((will be filled in by the editorial staff))

References

[1] J. M. Tarascon, M. Armand, *Nature* **2001**, *414*, 359.
[2] J. Lu, Z. Chen, Z. Ma, F. Pan, L. A. Curtiss, K. Amine, *Nat. Nanotechnol.* **2017**, *12*, 90.
[3] J. W. Choi, D. Aurbach, *Nat. Rev. Mater.* **2016**, *1*, 16013.
[4] K. Amine, I. Belharouak, Z. Chen, T. Tran, H. Yumoto, N. Ota, S. T. Myung, Y. K. Sun, *Adv. Mater.* **2010**, *22*, 3052.
[5] L. Ji, Z. Lin, M. Alcoutlabi, X. Zhang, *Energy Environ. Sci.* **2011**, *4*, 2682.
[6] X. Duan, J. Xu, Z. Wei, J. Ma, S. Guo, H. Liu, S. Dou, *Small Methods* **2017**, *1*, 1700156.

[7] X. Deng, Z. Wei, C. Cui, Q. Liu, C. Wang, J. Ma, *J. Mater. Chem. A.* **2018**, DOI: 10.1039/C7TA11301C.

[8] M. Mao, C. Cui, M. Wu, M. Zhang, T. Gao, X. Fan, J. Chen, T. Wang, J. Ma, C. Wang, *Nano Energy* **2018**, *45*, 346.

[9] C. Shen, G. Hu, L. Z. Cheong, S. Huang, J. G. Zhang, D. Wang, *Small Methods* **2018**, *2*, 1700298.

[10] P. G. Bruce, S. A. Freunberger, L. J. Hardwick, J. M. Tarascon, *Nat. Mater.* **2012**, *11*, 19.

[11] D. Lin, Y. Liu, Y. Cui, *Nat. Nanotechnol.* **2017**, *12*, 194.

[12] J. Hu, J. Tian, C. Li, *ACS Appl. Mater. Inter.* **2017**, *9*, 11615.

[13] Y. Xie, L. Fang, H. Cheng, C. Hu, H. Zhao, J. Xu, J. Fang, X. Lu, J. Zhang, *J. Mater. Chem. A.* **2016**, *4*, 15612.

[14] C. Hu, H. Chen, Y. Xie, L. Fang, J. Fang, J. Xu, H. Zhao, J. Zhang, *J. Mater. Chem. A.* **2016**, *4*, 18284.

[15] Z. Liang, Q. Zou, Y. Wang, Y.-C. Lu, *Small Methods* **2017**, *1*, 1700150.

[16] Q. Liu, Z. Chang, Z. Li, X. Zhang, *Small Methods* **2018**, *2*, 1700231.

[17] J. Zhang, H. Huang, J. Bae, S.-H. Chung, W. Zhang, A. Manthiram, G. Yu, *Small Methods* **2018**, *2*, 1700279.

[18] R. Fang, S. Zhao, P. Hou, M. Cheng, S. Wang, H. M. Cheng, C. Liu, F. Li, *Adv. Mater.* **2016**, *28*, 3374.

[19] W. Chen, T. Qian, J. Xiong, N. Xu, X. Liu, J. Liu, J. Zhou, X. Shen, T. Yang, Y. Chen, *Adv. Mater.* **2017**, *29*, 1605160.

[20] J. Xu, J. Ma, Q. Fan, S. Guo, S. Dou, *Adv. Mater.* **2017**, *29*, 1606454.

[21] H. Kim, G. Jeong, Y.-U. Kim, J.-H. Kim, C.-M. Park, H.-J. Sohn, *Chem. Soc. Rev.* **2013**, *42*, 9011.

[22] W. Xu, J. Wang, F. Ding, X. Chen, E. Nasybutin, Y. Zhang, J.-G. Zhang, *Energy Environ. Sci.* **2014**, *7*, 513.

[23] H. Song, H. Deng, C. Li, N. Feng, P. He, H. Zhou, *Small Methods* **2017**, *1*, 1700135.

[24] W. Li, H. Yao, K. Yan, G. Zheng, Z. Liang, Y. M. Chiang, Y. Cui, *Nat. Commun.* **2015**, *6*, 7436.

[25] D. Lu, Y. Shao, T. Lozano, W. D. Bennett, G. L. Graff, B. Polzin, J. Zhang, M. H. Engelhard, N. T. Saenz, W. A. Henderson, *Adv. Energy Mater.* **2015**, *5*, 1400993.

[26] C. P. Yang, Y. X. Yin, S. F. Zhang, N. W. Li, Y. G. Guo, *Nat. Commun.* **2015**, *6*, 8058.

[27] A. C. Kozen, C. F. Lin, A. J. Pearse, M. A. Schroeder, X. G. Han, L. B. Hu, S. B. Lee, G. W. Rubloff, M. Noked, *ACS Nano* **2015**, *9*, 5884.

[28] D. Aurbach, Y. Cohen, **1996**, *143*, 3525.

[29] M. S. Whittingham, *Proc. IEEE* **2012**, *100*, 1518.

[30] X. B. Cheng, C. Yan, H. J. Peng, J. Q. Huang, S. T. Yang, Q. Zhang, *Energy Storage Mater.* **2018**, *10*, 199.

[31] J. Zheng, M. H. Engelhard, D. Mei, S. Jiao, B. J. Polzin, J.-G. Zhang, W. Xu, *Nat. Energy* **2017**, *2*, 17012.

[32] X. Q. Zhang, X. B. Cheng, X. Chen, C. Yan, Q. Zhang, *Adv. Funct. Mater.* **2017**, *27*, 1605989.
[33] H. Ota, K. Shima, M. Ue, J.-i. Yamaki, *Electrochim. Acta* **2004**, *49*, 565.
[34] F. Ding, W. Xu, G. L. Graff, J. Zhang, M. L. Sushko, X. Chen, Y. Shao, M. H. Engelhard, Z. Nie, J. Xiao, X. Liu, P. V. Sushko, J. Liu, J.-G. Zhang, *J. Am. Chem. Soc.* **2013**, *135*, 4450.
[35] Z. Lin, Z. Liu, W. Fu, N. J. Dudney, C. Liang, *Adv. Funct. Mater.* **2013**, *23*, 1064.
[36] J. Qian, W. Xu, P. Bhattacharya, M. Engelhard, W. A. Henderson, Y. Zhang, J. G. Zhang, *Nano Energy* **2015**, *15*, 135.
[37] W. Zhou, S. Wang, Y. Li, S. Xin, A. Manthiram, J. B. Goodenough, *J. Am. Chem. Soc.* **2016**, *138*, 9385.
[38] Z. Tu, Y. Kambe, Y. Lu, L. A. Archer, *Adv. Energy Mater.* **2014**, *4*, 155.
[39] D. Lin, Y. Liu, Z. Liang, H.-W. Lee, J. Sun, H. Wang, K. Yan, J. Xie, Y. Cui, *Nat. Nanotechnol* **2016**, *11*, 626.
[40] Y. Zhang, B. Liu, E. Hitz, W. Luo, Y. Yao, Y. Li, J. Dai, C. Chen, Y. Wang, C. Yang, H. Li, L. Hu, *Nano Research* **2017**, *10*, 1356.
[41] F. Shen, X. Han, F. Zhang, Y. Zheng, Z. Fan, Z. Li, Z. Sun, Y. Xuan, B. Zhao, Z. Lin, X. Gui, Y. Cheng, C. Niu, *Energy Storage Mater.* **2018**, DOI: 10.1016/j.ensm.2018.02.005.
[42] S.-S. Chi, Y. Liu, W.-L. Song, L.-Z. Fan, Q. Zhang, *Adv. Funct. Mater.* **2017**, *27*, 1700348.
[43] J. G. L. L. Lu, J. N. Yang, S. M. Chen, H. B. Yao, F. Zhou, S. H. Yu, *Nano Lett.* **2016**, *16*, 4431.
[44] Q. Li, S. Zhu, Y. Lu, *Adv. Funct. Mater.* **2017**, *27*, 1606422.
[45] Q. Yun, Y.-B. He, W. Lv, Y. Zhao, B. Li, F. Kang, Q.-H. Yang, *Adv. Mater.* **2016**, *28*, 6932.
[46] D. Wang, Y. Yu, J. Zhu, S. Liu, D. A. Muller, H. D. Abruña, *Nano Lett.* **2015**, *15*, 1343.
[47] L. Sun, C.-L. Chien, P. C. Searson, *Chem. Mater.* **2004**, *16*, 3125.
[48] X.-B. Cheng, R. Zhang, C.-Z. Zhao, Q. Zhang, *Chem. Rev.* **2017**, *117*, 10403.
[49] C. Yang, K. Fu, Y. Zhang, E. Hitz, L. Hu, *Adv. Mater.* **2017**, *29*, 1701169.
[50] K. Yan, Z. Lu, H. W. Lee, F. Xiong, P. C. Hsu, Y. Li, J. Zhao, S. Chu, Y. Cui, *Nat. Energy* **2016**, *1*, 16010.
[51] C. Yang, Y. Yao, S. He, X. Hua, E. Hitz, L. Hu, *Adv. Mater.* **2017**, *29*, 1702714.
[52] S. H. Wang, Y. X. Yin, T. T. Zuo, W. Dong, J. Y. Li, J. L. Shi, C. H. Zhang, N. W. Li, C. J. Li, Y. G. Guo, *Adv. Mater.* **2017**, *29*, 1703729.
[53] N.-W. Li, Y.-X. Yin, C.-P. Yang, Y.-G. Guo, *Adv. Mater.* **2016**, *28*, 1853.

We present the electrochemical etching method to prepare the 3D Cu with uniform and compact porous network. As current collector of Li metal anode, the 3D Cu with large internal surface area and enhanced mechanical property can effectively accommodate Li metal and suppress Li dendrite growth to achieve a high performance of Li-metal battery.

Keyword：electrochemical etching, 3D porous copper, Cu-Zn alloy, compact structure, Li metal batteries

Heng Zhao, Danni Lei, Yan-Bing He*,Yifei Yuan, Qinbai Yun, Bin Ni, Wei Lv, Baohua Li, Quan-Hong Yang, Feiyu Kang and Jun Lu*
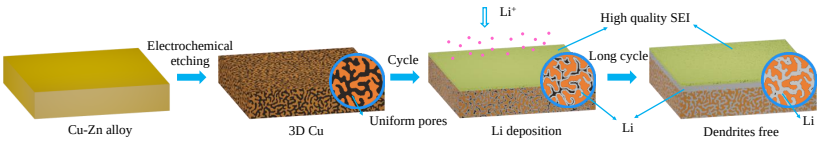
Compact 3D Copper with Uniform Porous Structure Derived by Electrochemical dealloying as Dendrite-free Lithium Metal Anode Current Collector